Available online at www.sciencedirect.com
SCIENCE DIRECT
Polymer 47 (2006) 6072–6080
polymer
www.elsevier.com/locate/polymer

Synthesis of amphiphilic graft copolymer with hydrophilic poly(acrylic acid) backbone and hydrophobic polystyrene side chains

Dan Peng, Xiaohuan Zhang, Xiaoyu Huang*

Key Laboratory of Organofluorine Chemistry, Shanghai Institute of Organic Chemistry, Chinese Academy of Sciences, 354 Fenglin Road, Shanghai 200032, PR China

Received 9 April 2006; received in revised form 12 June 2006; accepted 18 June 2006
Available online 10 July 2006

Abstract

A series of well-defined amphiphilic graft copolymers consisting hydrophilic poly(acrylic acid) backbones and hydrophobic polystyrene side chains were synthesized by successive atom transfer radical polymerization (ATRP) followed by hydrolysis of poly(methoxymethyl acrylate) (PMOMA) backbone. Grafting-from strategy was employed for the synthesis of graft copolymers with narrow molecular weight distribution. Hydrophobic side chains were connected to the backbone through stable C–C bonds. The backbone can be easily hydrolyzed with HCl without affecting hydrophobic side chains. This family of amphiphilic graft copolymers can form stable micelles in water. The critical micelle concentration was determined by fluorescence spectroscopy. The micellar morphologies and sizes were studied using transmission electron microscopy (TEM) and dynamic light scattering (DLS). The sizes of micelles were dependent on ionic strength, pH value and preparation conditions.

Keywords: Amphiphilic graft copolymer; Poly(acrylic acid); Macroinitiator

1. Introduction

Intensive interests on self-assembly of amphiphilic copolymers in water have been risen during the past decades [1–6] due to its potential applications in drug delivery systems [7–9], cosmetics products, coatings and the synthesis of nano-materials [10,11], etc. Studies of self-assembly behaviors of *block* copolymers in water have showed that the critical micelle concentration (*cmc*), micelle radius (R_h), and micelle aggregation number (N_{agg}) as well as micelle shape are influenced by the pH value of the solution, ionic strength, preparation conditions, copolymer concentration, molecular weight of copolymer and compositions of copolymer [12–14], whereas few researches focused on the behaviors of amphiphilic graft copolymers in water [15]. Recently, it was revealed that the architecture of copolymer also played an important role in determining the properties of micelle [16–18]. Graft copolymer possesses additional complexity in solution assembly resulting from its complicated and confined structure. So we can get more information about the controlling of micellar morphologies and design of new nano-materials through the study of the self-assembly of graft copolymers.

The studies of the self-assembly of graft copolymers were restrained due to the difficulty in the synthesis of well-defined graft copolymers with controlled molecular weights and low polydispersities. Generally, three strategies, including grafting-through, grafting-onto and grafting-from, can be used to synthesize graft copolymers [19]. With the development of atom transfer radical polymerization (ATRP) [20,21], the grafting-from technique has been widely used. By this method, side chains can be formed via ATRP which was initiated by the pendant initiation groups on the backbone. Lately, some groups have synthesized well-defined graft copolymers with hydrophobic backbone and hydrophilic side chains by this

* Corresponding author. Tel.: +86 21 54925310; fax: +86 21 64166128.
E-mail address: xyhuang@mail.sioc.ac.cn (X. Huang).

0032-3861/$ - see front matter © 2006 Elsevier Ltd. All rights reserved.
doi:10.1016/j.polymer.2006.06.045

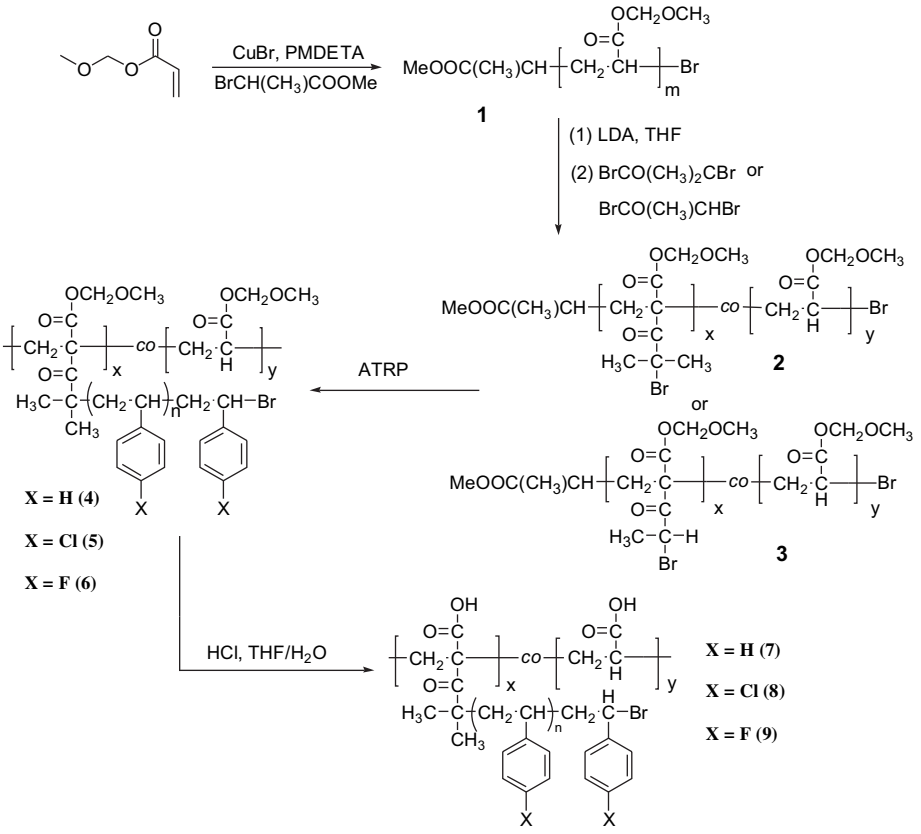

Scheme 1. Synthesis of amphiphilic graft copolymers.

way and their self-assembly behaviors have been explored [19,22]. However, there are only few reports about the synthesis of well-defined graft copolymers with hydrophilic backbone and hydrophobic side chains, as well as their self-assembly behaviors in aqueous solution [23,15].

In this paper, we report the synthesis of amphiphilic graft copolymers with hydrophilic poly(acrylic acid) backbone and hydrophobic polystyrene side chains (Scheme 1). The molecular weights of the backbone and the side chains were both controllable, and their polydispersities were kept low. Moreover, the self-assembly behaviors of these copolymers in water were preliminarily explored, the *cmc* was measured while the morphologies and sizes of the obtained micelles under different conditions were also studied with TEM and DLS.

2. Experimental

2.1. Materials

Styrene (St, Aldrich, 99%) was washed with 5% aqueous NaOH solution to remove inhibitor, and then with water, dried over $MgSO_4$ and distilled twice over CaH_2 under reduced pressure. *p*-Chloro-styrene (*p*-Cl-St, Aldrich, 99%) and *p*-fluoro-styrene (*p*-F-St, Aldrich, 99%) were distilled twice over CaH_2 under reduced pressure. Copper(I) bromide (CuBr, Aldrich, 98%) was purified by stirring overnight over CH_3CO_2H at room temperature, followed by washing the solid with ethanol, diethyl ether and acetone prior to drying at 40 °C under vacuum for 1 day. Diisopropylamine (Aldrich, 99.5%) was dried over KOH for several days followed by distilling from CaH_2 under N_2 atmosphere. Tetrahydrofuran (THF) was dried over CaH_2 for several days and distilled from sodium and benzophenone under N_2 atmosphere. *N*,*N*,*N*′,*N*′,*N*″-pentamethyldiethylenetriamine (PMDETA, Aldrich, 99%), methyl 2-bromopropionate (2-MBP, Acros, 99%), *n*-butyllithium (*n*-BuLi, Aldrich, 1.6 M in hexane), and α-bromoisobutyryl bromide (TCI, 98%) were used as received. Chloromethyl methyl ether was synthesized according to the previous literature [24].

2.2. Measurements

FT-IR spectra were recorded on a Nicolet AVATAR-360 FT-IR spectrophotometer with 4 cm^{-1} resolution. All ^1H NMR and ^{13}C NMR analyses were performed on a Varian Mercury 300 spectrometer (300 MHz) in $CDCl_3$ and with TMS (^1H NMR) and $CDCl_3$ (^{13}C NMR) as internal standard. Bromine content was determined by titration with $Hg(NO_3)_2$. Relative molecular weights and molecular weight distributions were measured by gel permeation chromatography (GPC) system equipped with a Waters 1515 Isocratic HPLC pump, a Waters 2414 refractive index detector (RI), a Waters 2487 dual absorbance detector and a set of Waters Styragel columns (HR3, HR4 and HR5, 7.8 × 300 mm). GPC measurements were carried out at 35 °C using THF as eluent with a 1.0 mL/min flow rate. The system was calibrated with polystyrene standards.

Steady-state fluorescent spectra were recorded on a Perkin–Elmer LS55 spectrofluorometer with the band width of 15 nm for excitation and 3 nm for emission. For emission spectra, λ_{ex} was 339 nm. TEM images were obtained using a Philips CM120 instrument operated at 80 kV. DLS was measured by an ALV/SP-125 LLS spectrometer equipped with an ALV-5000 multi-τ digital time correlator and a ADLAS DPY 425 II solid-state laser (400 MW output power at $\lambda = 632$ nm).

2.3. Synthesis of methoxymethyl acrylate (MOMA)

Triethylamine (30 mL, 216 mmol) and acrylic acid (13 mL, 189 mmol) were added to 200 mL dry dichloromethane at room temperature. Next, chloromethyl methyl ether (15 mL, 200 mmol) was added dropwise and the solution was stirred at room temperature until TLC showed the completion of the reaction. The solvent was removed by rotary evaporation and the residue was purified by distillation under reduced pressure to give the product (16.7826 g, 73% yield). FT-IR (film): ν (cm^{-1}): 3003 (=C–H), 2960 (–C–H), 1732 (C=O), 1299, 1264, 1202, 1153, 1095, 1025 (C–O–C), 932. ^{1}H NMR ($CDCl_3$): δ (ppm): 3.50 (s, 3H, CH_3O), 5.33 (s, 2H, COOCH_2O), 5.90 and 6.50 (dd, 1H, CH_2=CH), 6.17 (dd, 1H, CH_2=CH).

2.4. Polymerization of MOMA by ATRP

PMOMA **1** was prepared by ATRP of MOMA initiated by 2-MBP. A typical procedure is listed as follows: to a 25 mL Schlenk flask (flame-dried under vacuum just before use) sealed with a rubber septum, CuBr (0.2355 g, 1.65 mmol), MOMA (5 mL, 42.8 mmol), PMDETA (0.34 mL, 1.65 mmol) and 2-MBP (0.18 mL, 1.65 mmol) were charged. The flask was degassed by three cycles of freeze–pump–thaw, and then immersed in an oil bath thermostated at 50 °C for 2.5 h. THF was added to dissolve the viscous crude product and the solution was filtered through a short Al_2O_3 column to remove the catalyst. The resulting solution was concentrated and precipitated into hexane. The precipitation was dried under reduced pressure to obtain 3.8859 g glassy solid of 78% yield, $M_n = 3600$, $M_w/M_n = 1.14$. FI-IR (film): ν (cm^{-1}): 2957 (–C–H), 1740 (C=O), 1144, 1088 (C–O–C), 925. ^{1}H NMR ($CDCl_3$): δ (ppm): 1.09 (d, 3H, CH_3CH), 1.37–1.60, 1.84–2.08 (br, 2H, meso CH_2–CH), 1.60–1.82 (br, 2H, racemo CH_2–CH), 2.23–2.52 (br, 1H, CH_2–CH), 3.40 (s, 3H, OCH_3), 4.25 (t, 1H, CHBr), 5.16 (s, 2H, COOCH_2O). ^{13}C NMR ($CDCl_3$): δ (ppm): 33.3–36.9 (CH_2CH), 41.4 (CH_2CH), 57.8 (–OCH_3), 90.6 (COOCH_2O), 173.9 (COOCH$_2$). EA: Br%: 2.21%.

2.5. Synthesis of PMOMA-Br macroinitiator

In a sealed 250 mL three-neck flask, dried THF (20 mL) and diisopropylamine (2.8 mL, 20.0 mmol) were added. Then, the solution was cooled to −78 °C and *n*-BuLi (1.6 M, 11.2 mL, 17.9 mmol) was added slowly. After 1 h, the mixture was treated with PMOMA (1.7553 g, $M_n = 3600$, $M_w/M_n = 1.14$) in 100 mL dried THF under −78 °C. The reaction lasted for 7 h. Next, α-bromoisobutyryl bromide (2.5 mL, 20.2 mmol) was introduced. After 4 h, the reaction was terminated by water. The organic phase was washed with water and brine, and dried over $MgSO_4$ overnight. After filtration, the solution was concentrated, and precipitated into hexane. The product was dried under vacuum to give yellow powder (1.2043 g, $M_n = 3300$, $M_w/M_n = 1.27$). FT-IR (film): ν (cm^{-1}): 2957, 1740, 1252, 1212, 1159, 1092 (C–O–C), 912. ^{1}H NMR ($CDCl_3$): δ (ppm): 1.0–3.3 (br, protons on PMOMA backbone), 1.97 (s, 6H, C(CH_3)$_2$Br), 3.50 (s, 3H, –OCH_3), 5.28 (s, 2H, COOCH_2O). EA: Br%: 8.83%. If the reactant was α-bromopropionyl bromide, we can find an additional peak at $\delta = 4.46$ ppm (s, CH(CH_3)Br). ^{13}C NMR ($CDCl_3$): δ (ppm): 19.1–21.2 (C(CH_3)$_2$Br), 25.5–37.2 (CH_2 on PMOMA backbone), 39.1, 41.2 (CH on PMOMA backbone), 47.9 (*tert-C* on PMOMA backbone), 54.9 (C(CH_3)$_2$Br), 57.8 (OCH_3), 90.8 (COOCH_2O), 170.5, 173.9 (O–C=O), 207.4 (C=O).

2.6. Synthesis of graft copolymer PMOMA-g-PS **4**

In a typical procedure, a dried 25 mL Schlenk flask was charged with CuBr (0.0092 g, 0.06 mmol), PMOMA-Br (0.0519 g, $M_n = 3300$, $M_w/M_n = 1.27$, Br% = 8.83%), St (3.6 mL, 31.3 mmol) and PMDETA (0.013 g, 0.06 mmol). The flask was degassed by three cycles of freeze–pump–thaw followed by immersing into an oil bath thermostated at 80 °C. After 15 h, the polymerization was terminated by putting the flask into liquid nitrogen. The reaction mixture was diluted by THF and filtered through an alumina column to remove the catalyst. After concentration, PMOMA-*g*-PS graft polymer **4d** was obtained by precipitation into methanol and dried under vacuum (0.1494 g, monomer conversion = 4.2%, $M_n = 25{,}000$, $M_w/M_n = 1.38$). FT-IR (film): ν (cm^{-1}): 3026, 2924, 1741, 1601, 1493, 1452, 1155, 1089, 1028, 757, 699. ^{1}H NMR ($CDCl_3$): δ (ppm): 1.38 (br, 2H, CH_2), 1.79 (br, 1H, CH), 2.32, 2.70 (CH on PMOMA backbone), 3.36 (s, 3H, OCH_3), 4.40 (br, 1H, CH(Ph)Br), 5.16 (s, 2H, COOCH_2O), 6.54, 7.03 (br, 5H, C$_6H_5$).

2.7. Synthesis of graft copolymers PMOMA-g-P(p-Cl-St) **5** and PMOMA-g-P(p-F-St) **6**

The polymerization procedure was similar to that of PMOMA-*g*-PS. PMOMA-*g*-P(*p*-Cl-St) **5**: $M_n = 16{,}000$ g/mol, $M_w/M_n = 1.35$. ^{1}H NMR ($CDCl_3$): δ (ppm): 1.34 (br, 2H, CH_2), 1.61 (br, 1H, CH), 1.77–2.58 (CH_2CH on PMOMA backbone), 3.44 (s, 3H, OCH_3), 4.30 (br, 1H, CH(Ph)Br), 5.25 (s, 2H, COOCH_2O), 6.42, 7.07 (br, 4H, C$_6H_4$). PMOMA-*g*-P(*p*-F-St) **6**: $M_n = 14{,}000$ g/mol, $M_w/M_n = 1.32$. ^{1}H NMR ($CDCl_3$): δ (ppm): 1.30 (br, 2H, CH_2), 1.59 (br, 1H, CH), 1.74–2.46 (CH_2CH on PMOMA backbone), 3.32 (s, 3H, OCH_3), 5.11 (s, 2H, COOCH_2O), 6.37, 6.69 (br, 4H, C$_6H_4$).

2.8. Hydrolysis of graft copolymer containing PMOMA backbone

The graft polymer was dissolved in THF and treated with excess 1 M HCl for 2 h at room temperature. The reaction mixture was washed with water until the aqueous phase became neutral and then with brine and dried over $MgSO_4$. After filtration, the solution was concentrated and precipitated into hexane. The final white solid was dried under vacuum. PAA-*g*-PS **7**: FT-IR (film): ν (cm^{-1}): 3400, 3026, 2925, 2850, 1701, 1601, 1493, 1452, 757, 698. ^{1}H NMR ($CDCl_3$): δ (ppm): 0.80 (s, 6H, C(CH_3)$_2$), 1.38 (br, 2H, CH_2), 1.79 (br, 1H, C*H*), 2.32, 2.70 (C*H* on PAA backbone), 4.40 (br, 1H, C*H*(Ph)Br), 6.54, 7.03 (br, 5H, C_6H_5). PAA-*g*-P(*p*-Cl-St) **8**: ^{1}H NMR ($CDCl_3$): δ (ppm): 1.17–1.52 (br, 2H, CH_2), 1.53–1.99 (br, 1H, C*H*), 6.43, 7.08 (br, 4H, C_6H_4). PAA-*g*-P(*p*-F-St) **9**: ^{1}H NMR ($CDCl_3$): δ (ppm): 1.38 (br, 2H, CH_2), 1.66 (br, 1H, C*H*), 6.44, 6.78 (br, 4H, C_6H_4).

2.9. Determination of critical micelle concentration

We used pyrene as fluorescence probe. The acetone solution of pyrene (6 mg/100 mL, 2.97×10^{-4} mol/L) was added to water until the concentration of pyrene reached 5×10^{-7} mol/L. Next, different amounts of polymer solutions in THF (1 mg/mL) were added to water containing pyrene. All fluorescence spectra were recorded at 25 °C.

2.10. TEM and DLS studies

Two methods were used to prepare micelles. In the first way, the amphiphilic graft copolymer solution in THF (1 mg/mL) was added dropwise to water with vigorous stirring until the final concentration was 0.05 mg/mL. The solution was stirred for another several hours for the evaporation of THF. In the second way, water was added slowly to the copolymer solution in DMF with vigorous stirring until the solution appears cloudy and the organic solvent was removed by dialysis.

For TEM studies, a drop of micellar solution was deposited on an electron microscopy copper grid coated with carbon film and the water evaporated at room temperature overnight before TEM studies. For DLS studies, both the micellar solutions were filtered through a membrane filter with a nominal pore size of 0.45 μm.

3. Results and discussion

3.1. Synthesis of PMOMA backbone

Since we designed PAA-*g*-PS as the target polymer, we should choose a suitable poly(acrylate) backbone which can be readily hydrolyzed under mild conditions. *tert*-Butyl acrylate is a good choice [19,22], since it can be easily transformed to acrylic acid with CF_3COOH. But we found that it was difficult to introduce ATRP initiation groups to PtBA backbone that might be due to steric effect. As we know, methoxymethyl substituted ester is easy to be hydrolyzed into acrylic acid under mild acidic conditions while without steric effect. Then, methoxymethyl acrylate was selected as the monomer to synthesize the backbone.

PMOMA with low molecular weight distribution (PDI < 1.25) was obtained via ATRP with 2-MBP as initiator, using CuBr as catalyst and PMDETA as ligand. The polymerization was carried out at 50 °C with relatively high conversion (≥60%, Table 1). The molecular weight of PMOMA can be adjusted by regulating the feed ratio of monomer to initiator and coincided with the theoretical molecular weight ($M_{n,th}$) considering experimental errors.

^{1}H NMR spectrum of PMOMA is shown in Fig. 1. The peaks of the double bond protons ($\delta = 5.90$, 6.17 and 6.50 ppm) disappeared and the poly(acrylate) backbone signals arose at $\delta = 1.37$–2.52 ppm. The peak 'a' belonged to the protons of CH_3 of the initiation group at one end and the peak 'f' was attributed to the proton of C*H*Br at the other end. The two peaks confirmed ATRP mechanism of the polymerization. The content of bromine, which is located at the end of PMOMA chain, was determined by titration with mercuric nitrate (Br% in Table 1).

3.2. Synthesis of macroinitiator PMOMA-Br

In previous literature [19,22], graft copolymers prepared by ATRP normally had a hydrophobic backbone and hydrophilic side chains because the researchers utilized the ester groups on the backbone and converted them to halogen-containing ATRP initiation groups. To retain ester groups on the backbone so that they can be turned into hydrophilic carboxylic groups via hydrolysis, we used a completely new method to connect the ATRP initiation groups to the α-carbon of the ester groups using LDA and α-bromoisobutyryl bromide or α-bromopropionyl bromide as shown in Scheme 1. By this approach,

Table 1
Polymerization of MOMA by ATRP[a]

PMOMA	[MOMA]:[2-MBP]	T (°C)	t (h)	$M_{n,th}$ (g/mol)	M_n[b] (g/mol)	M_w/M_n[b]	Yield (%)	Br%[c]
1a	26:1	50	2.5	3000	3600	1.14	78	2.21
1b	53:1	50	8.5	6100	6600	1.10	60	0.62
1c	78:1	50	12	9000	11,000	1.21	69	–

[a] Feed ratio: [CuBr]:[PMDETA]:[2-MBP] = 1:1:1.
[b] Measured by GPC.
[c] Determined by titration with $Hg(NO_3)_2$.

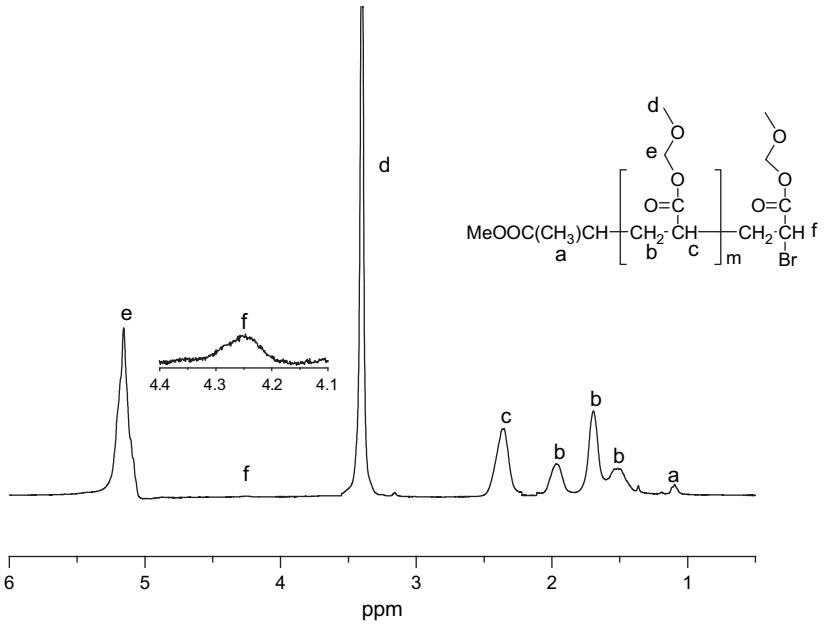

Fig. 1. ^{1}H NMR spectrum of PMOMA **1**.

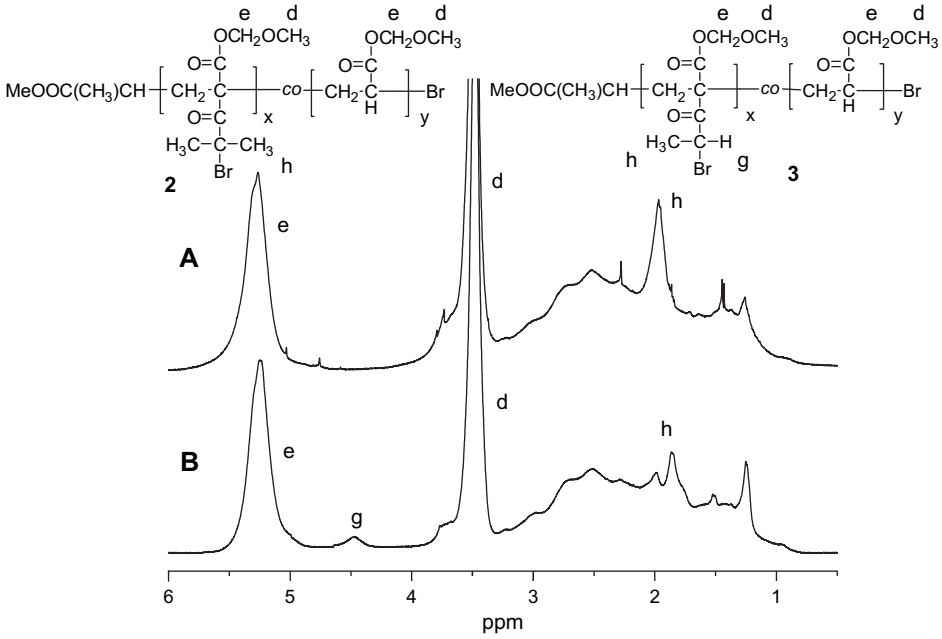

Fig. 2. ^{1}H NMR spectra of macroinitiator **2** (A) and macroinitiator **3** (B).

we successfully transformed PMOMA homopolymer into macroinitiator and ATRP initiation groups were connected to the backbone through stable C−C bonds instead of C−O bonds.

Fig. 2(A) and (B) showed ^{1}H NMR spectra of macroinitiators **2** and **3** with different initiation groups. We can find a new peak at 4.46 ppm (peak a) in Fig. 2(B) when the macroinitiator **3** was made from α-bromopropionyl bromide; but there is no peak at that position in ^{1}H NMR of macroinitiator **2** made from α-bromoisobutyryl bromide in Fig. 2(A). So we can assign this peak to the proton of $-CH(CH_3)Br$ of the newly introduced ATRP initiation groups. Moreover, a new peak at 207.4 ppm, which belonged to the keton carbon of $-CO(CH_3)_2Br$, was found in ^{13}C NMR spectrum of macroinitiators **2** and **3** as compared with that of PMOMA.

The changes in NMR spectra and the increase of Br% of macroinitiator (2.21−8.83% for **2a** and 0.62−11.25% for **2b**, listed in Table 2) assured the successful introduction of ATRP initiation groups. Considering the effectiveness of organic reactions, it was impossible to introduce ATRP initiation groups to every repeating unit. From the results of Br% of macroinitiator **2**, we can obtain the approximate graft efficiency: 1/7 for **2a** and 1/5 for **2b**, which means ATRP initiation groups were introduced to one-seventh or one-fifth

Table 2
Characterization of macroinitiators **2a** and **2b**

Macroinitiator	M_n (g/mol)	M_w/M_n	Br%	Graft efficiency
2a[a]	3300	1.27	8.83	1/7
2b[b]	4200	1.23	11.25	1/5

[a] Compound **2a** was prepared from **1a**.
[b] Compound **2b** was prepared from **1b**.

of repeating units of PMOMA backbone. It should be noteworthy that GPC results calibrated with linear PS showed a minor decrease of the molecular weight after linear PMOMA **1** was converted to branched macroinitiator **2**. The more introduction of ATRP initiation groups led to the more decrease of molecular weight.

3.3. Graft copolymerization of St, p-Cl-St and p-F-St

Table 3 presented the results of graft copolymerization of St, *p*-Cl-St and *p*-F-St initiated by macroinitiators **2a** and **2b**. We can find that molecular weights increased with the extending of the polymerization time, which is characteristic of ATRP. All graft copolymers showed unimodal GPC curves with low molecular weight distributions at low conversion. If the conversion was higher than 5%, shoulder signals were observed in GPC curves, which indicated the occurrence of intermolecular coupling reactions. It seems that a high feed ratio of monomer to initiator and a low conversion of monomer were necessary to suppress undesirable side reactions, and therefore to obtain the well-defined graft copolymers as reported in previous work [19]. Due to the very low concentration of macroinitiator, the graft polymerization was slow as compared with conventional ATRP reactions [19]. The rates of polymerization increased with the sequence *p*-F-St < St < *p*-Cl-St, which was coinciding with the results of ATRP of the above monomers initiated by benzyl bromide [25].

Table 3
Synthesis of graft copolymers initiated by macroinitiators **2a** and **2b**

Copolymer	Monomer	Time (h)	Conversion (%)	M_n[c] (g/mol)	M_w/M_n[c]	$N_{MOMA}/N_{X\text{-}St}$[d]
4a[a]	St	5	1.3	13,000	1.34	1/6
4b[a]	St	6	1.8	17,000	1.36	1/8
4c[a]	St	10	3.9	21,000	1.38	1/10
4d[a]	St	15	4.2	25,000	1.38	1/12
4e[b]	St	6	1.9	15,000	1.42	1/5
5[b]	*p*-Cl-St	3	1.8	16,000	1.35	1/4
6[b]	*p*-F-St	24	1.5	14,000	1.32	1/5

[a] Initiated by **2a**, [St]:[Br]:[CuBr]:[PMDETA] = 500:1:1:1.
[b] Initiated by **2b**, [X-St]:[Br]:[CuBr]:[PMDETA] = 500:1:1:1.
[c] Measured by GPC.
[d] Obtained by ^{1}H NMR.

Fig. 3(A) showed ^{1}H NMR spectrum of PMOMA-*g*-PS: the corresponding peaks of both backbone and side chains can be found. A new peak appeared at 4.40 ppm (peak i) in Fig. 3(A), which is the signal of proton of −C*H*(Ph)Br end group, also confirming ATRP mechanism. With the value of S_{e+d}/S_{phenyl} (S is the peak area), we can get the ratios of repeating units of backbone to the side chains ($N_{MOMA}/N_{X\text{-}St}$ in Table 3).

3.4. Hydrolysis of backbone

Hydrolysis was carried out under mild acidic conditions. After hydrolysis, we cannot find any trace of methoxymethyl

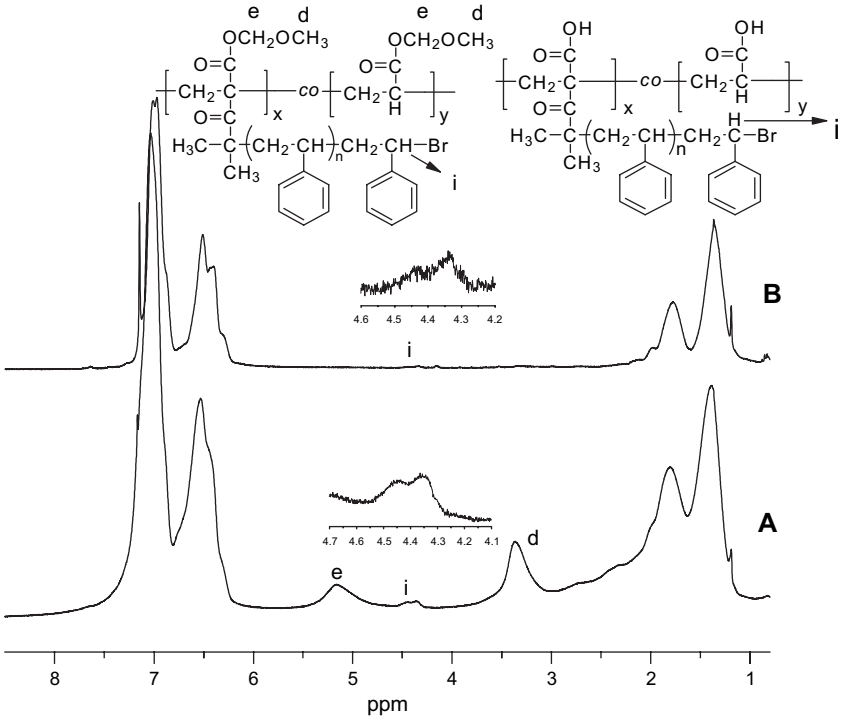

Fig. 3. ^{1}H NMR spectra of PMOMA-*g*-PS (A) and PAA-*g*-PS (B).

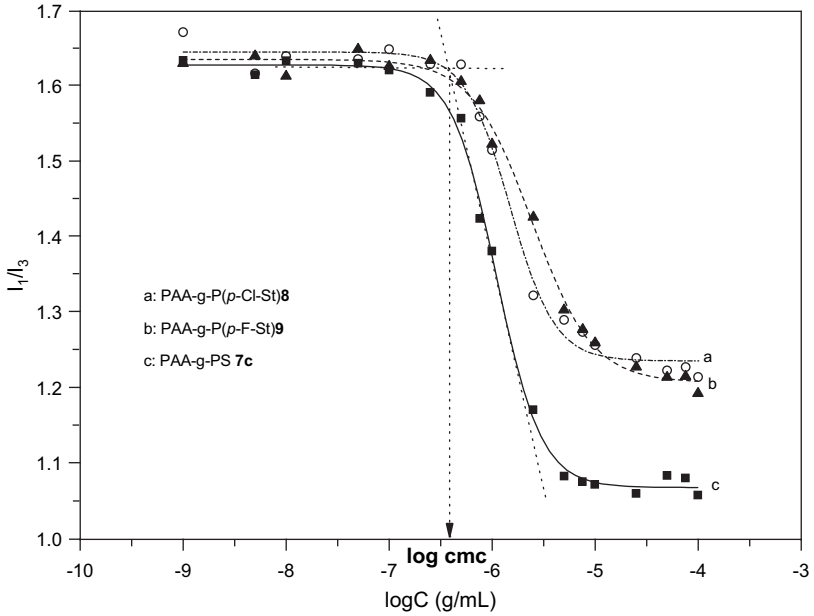

Fig. 4. Dependence of fluorescence intensity ratios of pyrene emission bands on the concentration of PAA-*g*-PS **7c**, PAA-*g*-P(*p*-Cl-St) **8** and PAA-*g*-P(*p*-F-St) **9**.

proton signals ($\delta = 3.36$ and 5.16 ppm) in ^{1}H NMR spectrum shown in Fig. 3(B). Also, we found a new broad peak of −COOH in FT-IR spectrum at 3400 cm^{-1} wavenumbers. All these evidences confirmed the complete hydrolysis of PMOMA and the formation of PAA backbone.

3.5. Measurement of critical micelle concentration

We examined the critical micelle concentrations of PAA-*g*-PS, PAA-*g*-P(*p*-Cl-St) and PAA-*g*-P(*p*-F-St) in aqueous solution by fluorescence technique using pyrene as probe [26–28]. This method is based on the sensitivity of the probe to the hydrophobicity and polarity of its micro-environment. In the presence of micelles, pyrene is solubilized within the interior of the hydrophobic part. As a result, the values of I_1/I_3 in the emission spectrum changed sharply. We plotted fluorescence peak intensity ratios (I_1/I_3) against the logarithm of polymer concentrations to determine *cmc* as the onset of micellization (Fig. 4).

As shown in Table 4, the values of *cmc* are around 10^{-7} g/mL which are very low compared with traditional surfactants or *block* copolymers [29]. The *cmc* values decreased with the increase of the contents of hydrophobic side chains (**7d** < **7c**). These low *cmc* values are related with the branched structure of graft copolymers and the asymmetric compositions since the percentage of hydrophobic side chains is up to 80%. With such low *cmc* values, amphiphilic graft copolymers can form highly stable micellar aggregates with low rates of dissociation *in vivo* [30].

Since the values of I_1/I_3 reflected the polarity of the micro-environment, we can get the polarity sequence of the hydrophobic side chains: P(*p*-Cl-St) ≈ P(*p*-F-St) > PS from Fig. 4.

Table 4
Critical micelles concentration of amphiphilic graft copolymers

Monomer	Copolymer	$N_{hydrophilic}/N_{hydrophobic}$	*cmc*
St	**7c**	1/10	3.72×10^{-7}
St	**7d**	1/12	3.02×10^{-7}
p-Cl-St	**8**	1/4	5.37×10^{-7}
p-F-St	**9**	1/5	6.03×10^{-7}

3.6. The effect of preparation conditions on micellar morphologies and sizes

We used two methods to prepare micellar solutions. The TEM and DLS results showed that the preparation conditions affected the micellar sizes. For graft copolymer PAA-*g*-PS **7d** (hydrolysis product of **4d**), the micelles formed by the first method were spheres with $\langle R_h \rangle = 70$ nm and PDI = 0.16, while the micelles prepared by the second method were not only spheres but also rods with $\langle R_h \rangle = 17$ nm and PDI = 0.24 (Fig. 5).

When polymer solution was added to water in the first method, the polarity of the environment of polystyrene increased quickly in a short time, which caused the abrupt decrease of entropy and increase of free energy, so the hydrophobic polystyrene side chains intended to aggregate to reduce the free energy. Because of the abrupt increase of free energy and the existence of much water, the exchanges between micelles and mono-chains were almost 'frozen' and big micelles were preferred to be formed. Fig. 6 also showed TEM images of sphere micelles formed by PAA-*g*-P(*p*-Cl-St), PAA-*g*-P(*p*-F-St) and PAA-*g*-PS **7b** with different weights using the first method. In the second method, the content of common solvent was high enough so that the free energy would not increase sharply and the exchanges between

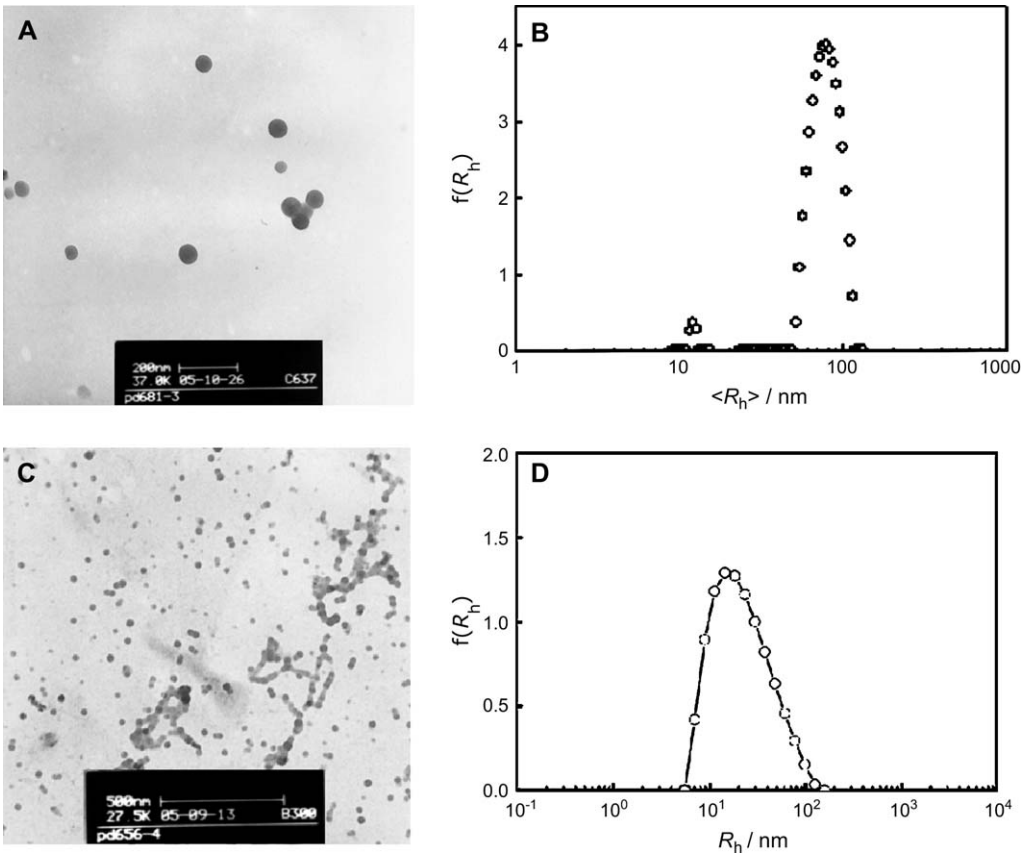

Fig. 5. TEM images (A), (C) and typical hydrodynamic radius distribution $f(R_h)$ (B), (D) of micelles of PAA-*g*-PS **7d** (A, B: prepared by the first method; C, D: prepared by the second method).

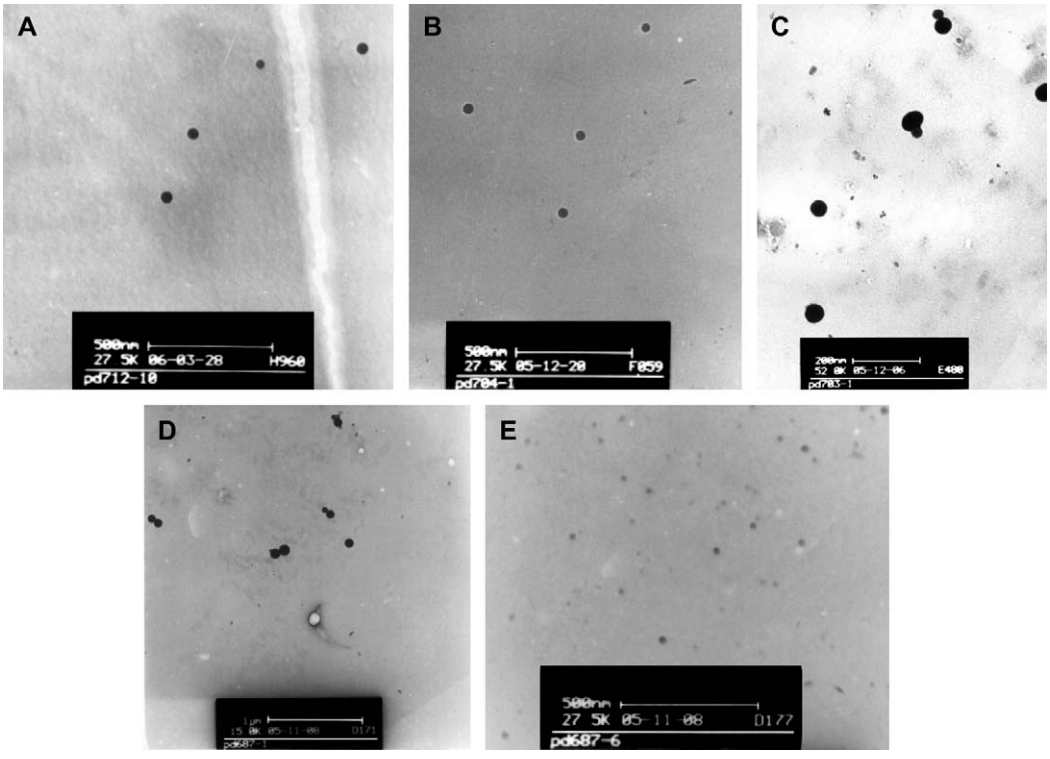

Fig. 6. TEM images of micelles of PAA-*g*-PS **7b** in water, $C = 2 \times 10^{-5}$ g/mL (A); PAA-*g*-P(*p*-Cl-St) **8** in water, $C = 2 \times 10^{-5}$ g/mL (B); PAA-*g*-P(*p*-F-St) **9** in water, $C = 2 \times 10^{-5}$ g/mL (C); PAA-*g*-PS **7b** in 1% NaCl solution, $C = 1 \times 10^{-5}$ g/mL (D) and PAA-*g*-PS **7b** in NaOH solution, pH = 12.33, $C = 2 \times 10^{-5}$ g/mL (E).

micelles and mono-chains were sufficient, which benefited the formation of smaller micelles.

3.7. The effect of ionic strength and pH on the micellar sizes

Since poly(acrylic acid) backbone is a kind of polyelectrolyte, the self-assembly behavior of PAA-*g*-PS in aqueous solution should be related with the ionic strength and pH values. We studied the micellar morphologies and sizes in NaCl solution and NaOH solution, respectively. Fig. 6(D) presented the TEM images of micelles of PAA-*g*-PS **7b** in 1% NaCl solution. With the increase of ionic strength, the sphere micelles became bigger (ca. 100 nm) than that in water (ca. 50 nm). It can be explained that Na^+ could screen the electronic repulsion among the hydrophilic poly(acrylic acid) backbones, so the hydrophobic side chains were easier to aggregate to form big micelles [15]. The addition of NaOH to water promoted the ionization of PAA and the charge density on the hydrophilic backbone increased, which prevented the aggregation of side chains, so the smaller micelles (ca. 20–30 nm, Fig. 6(E)) formed in basic aqueous solution compared with that in neutral solution [5].

4. Conclusion

In this paper, we demonstrated a new approach to synthesize well-defined amphiphilic graft copolymers with hydrophilic PAA backbone by ATRP and grafting-from technique. PAA-*g*-PS, PAA-*g*-P(*p*-Cl-St), and PAA-*g*-P(*p*-F-St) were obtained after easy hydrolysis of PMOMA backbone. This method can be extended to graft many other polymer blocks, which will be a significant progress for building amphiphilic graft copolymers.

These amphiphilic graft copolymers can form stable micelles in water. Preliminary studies showed that they have a low *cmc* values of about 10^{-7} g/mL. The shapes and sizes of micelles were found to be related with the micellar preparation methods. The sizes of micelles increased with the addition of NaCl to water and decreased at high pH values. These findings enriched the self-assembly studies of amphiphilic copolymer and were helpful for control of micellar shapes and sizes.

Acknowledgement

The authors thank the financial support from National Natural Science Foundation of China (grant no.: 20404017).

References

[1] Halperin A, Tirrell M, Lodge TP. Adv Polym Sci 1992;100:31.
[2] Zhang L, Eisenberg A. Science 1995;268:1728.
[3] Zhang L, Eisenberg A. J Am Chem Soc 1996;118:3168.
[4] Zhang L, Yu K, Eisenberg A. Science 1996;272:1777.
[5] Zhang L, Eisenberg A. Macromolecules 1996;29:8805.
[6] Zhang L, Bartels C, Yu Y, Shen H, Eisenberg A. Phys Rev Lett 1997; 79:5034.
[7] Ahmed F, Discher DE. J Control Release 2004;96:37.
[8] Pan D, Turner JL, Wooley KL. Chem Commun 2003;19:2400.
[9] Rosler AV, Guido WM, Klok HA. Adv Drug Deliv Rev 2001;53:95.
[10] Ikkala O, ten Brinke G. Science 2002;295:2407.
[11] Jeoung E, Galow TH, Schotter J. Langmuir 2001;17:6396.
[12] Forder C, Patrickios CC, Armes SP, Billingham NC. Macromolecules 1996;29:8160.
[13] Thurmond KB, Kowalewski T, Wooley KL. J Am Chem Soc 1997;119: 6656.
[14] Maskos M, Harris JR. Macromol Rapid Commun 2001;22:271.
[15] Ma Y, Cao T, Webber SE. Macromolecules 1998;31:1773.
[16] Cai Y, Tang Y, Armes SP. Macromolecules 2004;37:9728.
[17] Förster S, Plantenberg T. Angew Chem Int Ed 2002;41:688.
[18] Riess G. Prog Polym Sci 2003;28:1107.
[19] Zhang M, Breiner T, Mori H, Müller AHE. Polymer 2003;44:1449.
[20] Wang J, Matyjaszewski K. J Am Chem Soc 1995;117:5614.
[21] Matyjaszewski K, Xia J. Chem Rev 2001;101:2921.
[22] Cheng G, Böker A, Zhang M, Krausch G, Müller AHE. Macromolecules 2001;34:6883.
[23] Zhang H, Ruckenstein E. Macromolecules 2000;33:814.
[24] Harada R, Kondo H. Bull Chem Soc Jpn 1968;41:2521.
[25] Qiu J, Matyjaszewski K. Macromolecules 1997;30:5643.
[26] Kalyanasundaram K, Thomas J. J Am Chem Soc 1977;99:2039.
[27] Wilhelm M, Zhao C, Wang Y, Xu R, Winnik M, Mura J, et al. Macromolecules 1991;24:1033.
[28] Astafieva I, Zhong X, Eisenberg A. Macromolecules 1993;26:7339.
[29] Lavasanifar A, Samuel J, Kwon G. Colloids Surf B 2001;22:115.
[30] Allen C, Maysinger D, Eisenberg A. Colloids Surf B 1999;16:3.